การดันเข้าของฟันหน้าบนหกซี่ ด้วยหลักยึดหมุดฝังในกระดูก วิเคราะห์โดยวิธีไฟไนต์ เอลิเมนต์

Intrusion of Six Maxillary Anterior Teeth Using Mini-screw Anchorage: A Finite Element Study

ศุภรัสมิ์ ศักดากรกุล[1], วิรัช พัฒนาภรณ์[2], ชาย รังสิยากูล[3]
[1]นักศึกษาระดับบัณฑิตศึกษา สาขาวิชาทันตกรรมจัดฟัน คณะทันตแพทยศาสตร์ มหาวิทยาลัยเชียงใหม่
[2]ภาควิชาทันตกรรมจัดฟันและทันตกรรมสำหรับเด็ก คณะทันตแพทยศาสตร์ มหาวิทยาลัยเชียงใหม่
[3]ภาควิชาวิศวกรรมเครื่องกล คณะวิศวกรรมศาสตร์ มหาวิทยาลัยเชียงใหม่
Suparat Sakdakornkul[1], Virush Patanaporn[2], Chaiy Rungsiyakul[3]
[1]Graduate student, Division of Orthodontics, Department of Orthodontic and Pediatric Dentistry, Faculty of Dentistry, Chiang Mai University
[2]Department of Orthodontics and Pediatric Dentistry, Faculty of Dentistry, Chiang Mai University
[3]Department of Mechanical Engineering, Faculty of Engineering, Chiang Mai University

ชม. ทันตสาร 2562; 40(2) : 51-63
CM Dent J 2019; 40(2) : 51-63

Received: 23 January, 2018
Revised: 10 April, 2018
Accepted: 11 May, 2018

บทคัดย่อ

วัตถุประสงค์: เพื่อประเมินการกระจายความเครียดแบบวอนมิสเซส และการเคลื่อนที่ของฟันหน้าบนหกซี่ด้วยกลไกการดันเข้า 2 ชนิดด้วยหลักยึดหมุดฝังในกระดูก วิเคราะห์โดยวิธีไฟไนต์เอลิเมนต์

วิธีการ: สร้างแบบจำลองไฟไนต์เอลิเมนต์ของฟันหน้าบนหกซี่ พร้อมทั้งเอ็นยึดปริทันต์ และกระดูกเบ้าฟัน กลไกแบบที่ 1 จะใช้หลักยึดหมุดฝังในกระดูก 1 ตัว ฝังที่ระหว่างรากฟันตัดซี่กลางบน ให้แรงลัพธ์รวม 60 กรัม ที่ลวดเส้นหลักบริเวณระหว่างฟันตัดบนซี่กลาง กลไกแบบที่ 2 จะใช้หลักยึดหมุดฝังในกระดูก 2 ตัว ฝังที่ระหว่างรากฟันตัดซี่ข้าง

Abstract

Objectives: To evaluate the von Mises stress distribution and displacement of the six maxillary anterior teeth intruded with two patterns of mini-screw anchorage, analyzed by the finite element method.

Methods: A finite element model of six maxillary anterior teeth with periodontal ligament and alveolar bone was constructed. In anchorage pattern 1, one mini-screw was placed between the central incisors with a net force of 60 g applied to

Corresponding Author:

วิรัช พัฒนาภรณ์
ศาสตราจารย์ คลินิก, ภาควิชาทันตกรรมจัดฟันและทันตกรรมสำหรับเด็ก คณะทันตแพทยศาสตร์ มหาวิทยาลัยเชียงใหม่ 50200

Virush Patanaporn
Clinical Professor, Department of Orthodontic and Pediatric Dentistry, Faculty of Dentistry, Chiang Mai University, Chiang Mai 50200, Thailand
E-mail: ***vr167420@hotmail.com***

บนและฟันเขี้ยวบน ให้แรง 2 ข้าง ซ้ายและขวา รวม 60 กรัม ในแนวเฉียงที่ลวดเส้นหลักบริเวณฟันตัดซี่กลางบนและฟันตัดซี่ข้างบน ทำการวิเคราะห์การกระจายความเครียดและการเคลื่อนที่ของฟัน

ผลการศึกษา: ในกลไกแบบที่ 1 ความเครียดแบบวอนมิสเซสที่ฟันตัดซี่กลางมีค่าสูงกว่าที่ฟันตัดซี่ข้างและฟันเขี้ยว ในกลไกแบบที่ 2 การกระจายความเครียดแบบวอนมิสเซสที่ฟันตัดซี่กลางและฟันตัดซี่ข้างมีค่าสูงใกล้เคียงกันและมากกว่าที่ฟันเขี้ยว ในกลไกแบบที่ 1 ฟันทุกซี่ถูกดันเข้าพร้อมกับยื่นและเอียงออกมามากขึ้น ในกลไกแบบที่ 2 ฟันตัดซี่กลางถูกดันเข้าตามแนวแกนฟัน ในขณะที่ฟันตัดซี่ข้างและฟันเขี้ยวยื่นออกมาเล็กน้อย

สรุปผล: กลไกการดันเข้าของฟันหน้าบนหกซี่ เมื่อใช้หลักยึดหมุดฝังในกระดูก 2 ตัว มีการกระจายความเครียดไปยังฟันตัดบน สี่ซี่ และทำให้เกิดการเคลื่อนฟันในทิศทางดันเข้าได้ดีกว่าการใช้หลักยึดหมุดฝังในกระดูก 1 ตัว

คำสำคัญ: หลักยึดหมุดฝังในกระดูก การดันเข้าของฟันหน้าบน วิธีไฟไนต์เอลิเมนต์

the arch wire between the central incisors towards the mini-screw. In anchorage pattern 2, two mini-screws were placed between the lateral incisors and canines, left and right, with a net force of 60 g applied to the arch wire between the central and lateral incisors in an oblique direction towards the mini-screws. The stress distribution and the displacement of the teeth were analyzed.

Results: In anchorage pattern 1, the von Mises stress on the central incisors was greater than that on the lateral incisors or canines. In anchorage pattern 2, the von Mises stress distribution was greater on the central and lateral incisors than on the canines. In anchorage pattern 1, all teeth were intruded with proclination. In anchorage pattern 2, the central incisors were intruded along their long axes, whereas the lateral incisors and canines were slightly proclined.

Conclusions: The two-mini-screw pattern distributes stress in four incisors and displaces teeth closer to pure intrusion than the one-mini-screw pattern.

Keywords: mini-screw, intrusion of maxillary anterior teeth, finite element method

Introduction

Intrusion of anterior teeth is necessary for patients with deep overbite and gummy smile, Class II skeletal relationship and large vertical facial height.(1-3) Conventional methods for incisor intrusion, such as the utility arch, intrusion arch, and reverse curved arches, have adverse side effects, such as labial tipping of maxillary anterior teeth and extrusion of posterior teeth.(1,4,5) Therefore, mini-screws are widely used as anchorage to intrude the anterior teeth, because there is no side effect to the posterior teeth, the force is easy to control and no patient co-operation is needed.(4) Previous investigations have reported successful intrusion of maxillary anterior teeth using mini-screws with variety of mechanics.(5-8)

Nanda and Tosun(9) recommended two anchorage patterns for intrusion of the six maxillary anterior teeth, one placing one mini-screw between the central incisors and applying one force to intrude the teeth, the placing two mini-screws between the lateral incisors and canines, left and right, and applying two forces obliquely to intrude the teeth.

Intrusion of anterior teeth usually produces proclination, an unwanted side effect.[1,4,5] Inclination control is needed when one mini-screw is placed between the central incisors.[6,7] Two mini-screws with oblique direction of force has rarely been studied; only Park *et al*[10] reported that the stress distribution for the intrusion of the six mandibular anterior teeth was even, and pure intrusion occurred when the mini-screws were placed distal to the canine and the force applications were between the central and lateral incisors. Using mini-screw anchorage with an oblique force direction is of interest for the intrusion of the six maxillary anterior teeth.

The finite element method (FEM) is a simulation program which predicts how an object reacts to different stimuli based on its properties.[11,12] It is an accurate technique for analyzing structural stress. In orthodontics, the FEM provides quantitative data that can facilitate the understanding of physiological reactions happening within the dento-alveolar complex.

The purposes of this study were to investigate the pattern of von Mises stress distribution in the periodontal ligament (PDL) and the displacement of teeth using two anchorage patterns for the intrusion of the six maxillary anterior teeth, analyzed by FEM.

Materials and methods

Commercial maxillary model (Model-i21FE-400C; Nissin Dental Products, Kyoto, Japan) were scanned using a 3-D scanner to produce digital tooth images. The model of the anterior maxillary segment was constructed using SolidWorks software (Dassault Systèmes Americas, Waltham, Mass., USA). The model included the left and right maxillary central and lateral incisors and canines with a 0.2-mm linear thickness of PDL along the root surface.[13,14] The maxillary alveolar bone consisted of cancellous bone and 1.0-mm thickness of cortical bone.[15] After all bony, dental, and PDL structures were graphically represented, brackets were modeled with 0.022x0.028-in slots, a stainless-steel arch wire was modeled with the dimensions 0.017x0.025-in, and no play (no movement of a wire in a bracket slot) was assumed between the brackets and the arch wire. The properties of all materials simulated in this study were based on previous reports from the literature[16] (Table 1). Dental and bone materials were assumed to be homogeneous, isotropic, and linearly elastic. To represent the non-linear mechanical behavior of the PDL, parameters of the hyper-elastic instantaneous response[17] were used (Table 2).

After the model construction, discretization was performed, and boundary conditions of the anatomic structures were assigned, using Abaqus software (Dassault Systèmes Americas). The assembled model of the six maxillary anterior teeth with alveolar support was meshed into several small elements. Each element had six degrees of freedom

ตารางที่ 1 *คุณสมบัติของฟัน กระดูกทึบ กระดูกเนื้อโปร่ง และเหล็กไร้สนิม*[16]

Table 1 *Material properties of tooth, cortical and cancellous bone and stainless steel*[16]

Material	Young's modulus (MPa)	Poisson's ratio
Dentin	19613.3	0.15
Cortical bone	13700	0.26
Cancellous bone	1370	0.3
Stainless steel	200000	0.3

ตารางที่ 2 *คุณสมบัติของเอ็นยึดปริทันต์ ค่าสัมประสิทธิ์ลำดับที่สามของสมการอ็อกเด็น*[17]

Table 2 *Material properties of the PDL. The coefficients of the third order Ogden model.*[17]

i	μ_i	α_i	D_i
1	-24.4237016	1.99994222	4.87164332
2	15.8966494	3.99994113	0.00000000
3	8.56953079	-2.00005453	0.00000000

(three displacements and three rotations). The boundary conditions were assigned on the top and back of the model. The final model consisted of 3,312,844 elements and 792,987 nodes.

The interactions between the elements of different objects were tie contact interactions, in which phases from the different materials remained without relative displacement between them. The teeth had no contact and no friction between them.

In this model the x-axis represented the mesio-distal, the y-axis the occluso-gingival, and the z-axis the labio-palatal aspects (Figure 1).

In anchorage pattern 1, one mini-screw was placed between the central incisors, 8 mm above the CEJ. A net force of 60 g was applied to the middle of the arch wire between the central incisors, because Proffit *et al*[18] recommended an intrusive force of 10 g per single-rooted tooth. The force direction was upward along the contour of the teeth and gingiva towards the mini-screw, at about 80° to the occlusal

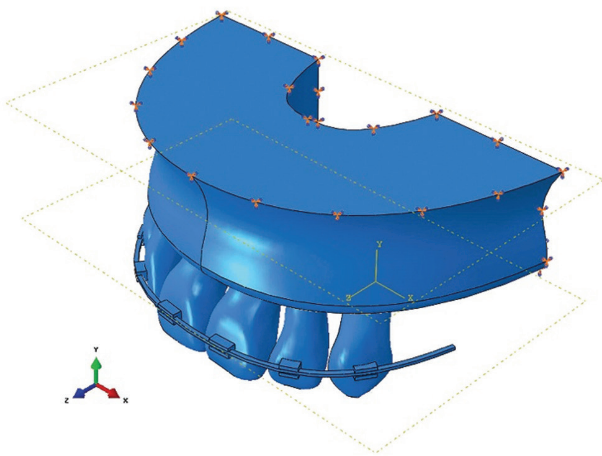

รูปที่ 1 *ระนาบอ้างอิงต่าง ๆ x คือด้านซ้าย, -x คือด้านขวา, y คือด้านบน, -y คือด้านล่าง, z คือด้านใกล้ริมฝีปาก, -z คือด้านใกล้เพดาน ลูกศรสีส้มแสดงเงื่อนไขขอบเขตทางด้านบนและด้านหลังของแบบจำลองไฟไนต์เอลิเมนต์*

Figure 1 *Reference planes: x=left; -x=right; y=superior; -y=inferior; z=labial; -z, palatal directions. Orange arrows show the boundary conditions at the top and back of the FE model.*

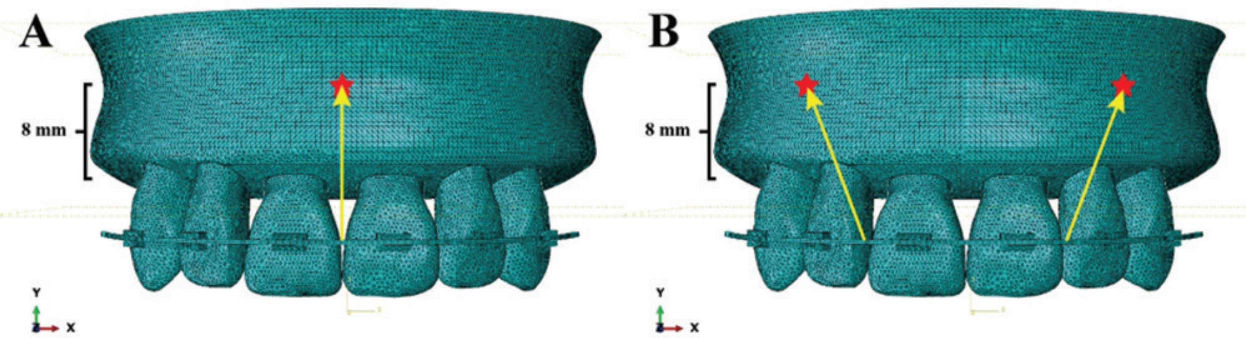

รูปที่ 2 *แบบจำลองไฟไนต์เอลิเมนต์ที่สร้างตาข่ายแล้ว แสดงตำแหน่งของหลักยึดหมุดฝังในกระดูก (รูปดาวสีแดง) และทิศทางของแรง (ลูกศรสีเหลือง)*

A) หลักยึดแบบที่ 1 ใช้หลักยึดหมุดฝังในกระดูก 1 ตัว ปักระหว่างฟันตัดซี่กลางบน และให้แรงจากหลักยึดหมุดฝังในกระดูกไปยังลวดเส้นหลักระหว่างฟันตัดซี่กลางบน

B) หลักยึดแบบที่ 2 ใช้หลักยึดหมุดฝังในกระดูก 2 ตัว ปักระหว่างฟันตัดซี่ข้างบนและฟันเขี้ยวบน ให้แรงจากหลักยึดหมุดฝังในกระดูกไปยังลวดเส้นหลักระหว่างฟันตัดซี่กลางบนและฟันตัดซี่ข้างบน

Figure 2 *Meshed FE models with mini-screw placement (red stars) and force direction (yellow arrows).*

A) Anchorage pattern 1: one mini-screw between the maxillary central incisors and a force applied from the main arch wire between the maxillary central incisors to the mini-screw.

B) Anchorage pattern 2: two mini-screws between the maxillary lateral incisors and canines and forces applied from the main arch wire between the maxillary central and lateral incisors.

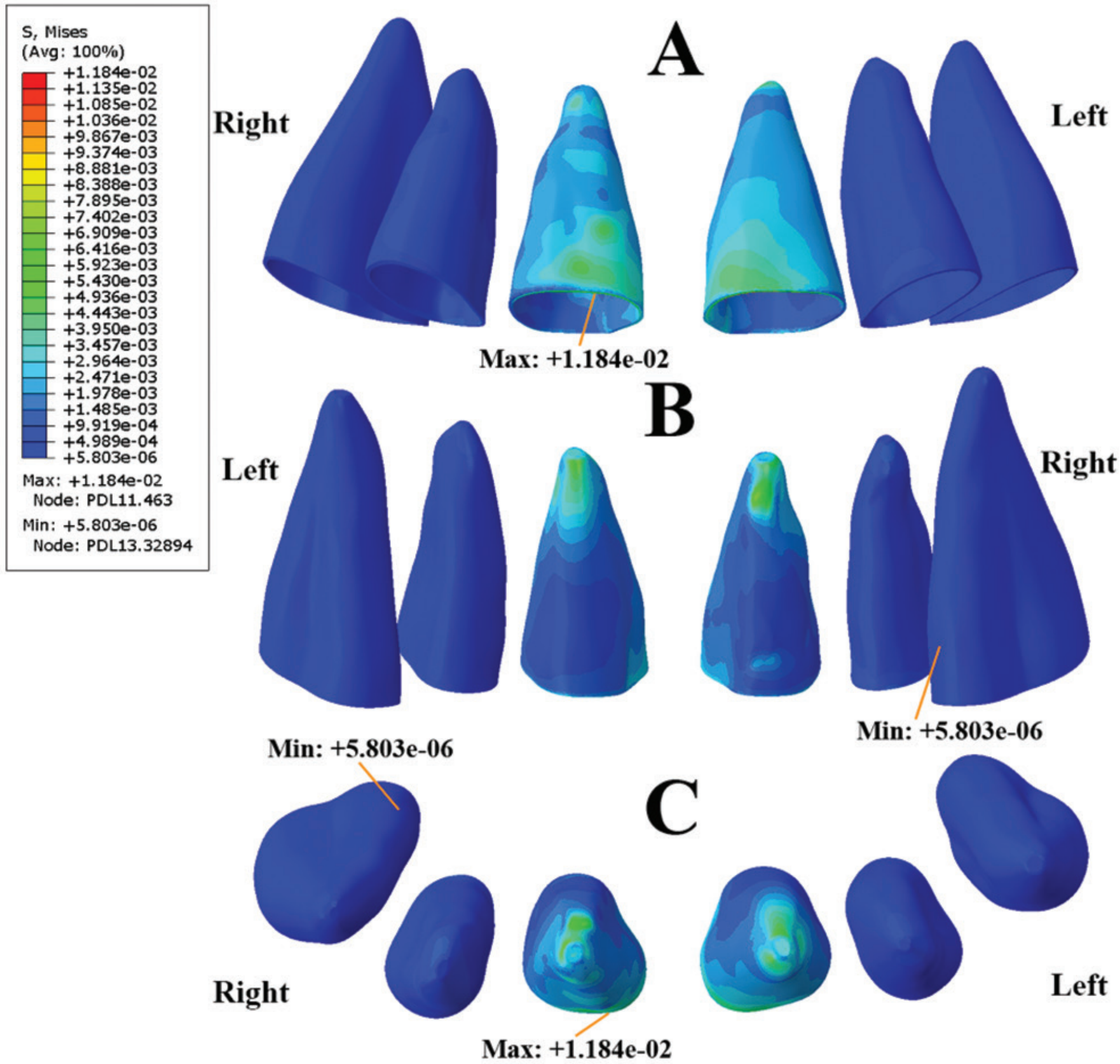

รูปที่ 3 *หลักยึดแบบที่ 1 แผนภาพสีแสดงการกระจายความเครียด เมื่อได้รับแรง 60 กรัม ด้านใกล้ริมฝีปาก (A) ด้านใกล้เพดาน (B) ด้านปลายราก (C)*

Figure 3 *Anchorage pattern 1, the color-coded map shows the distribution of stress of 60 g force: labial (A), palatal (B), and apical views (C).*

plane (Figure 2). In anchorage pattern 2, two mini-screws were placed between the lateral incisors and canines, left and right. A net force of 60 g, divided by two, applied to the arch wire between the lateral incisor and canine on each side in an oblique direction towards the mini-screw (Figures 2). The left force (FL) and right force (FR) were divided among the x, y and z axes. FL and FR were equal in magnitude, but FR-x was in the opposite direction to FLx.

The Abaqus software (Dassault Systèmes Americas) was used to analyze the von Mises stress distribution pattern and displacement for the intrusion of the six maxillary anterior teeth.

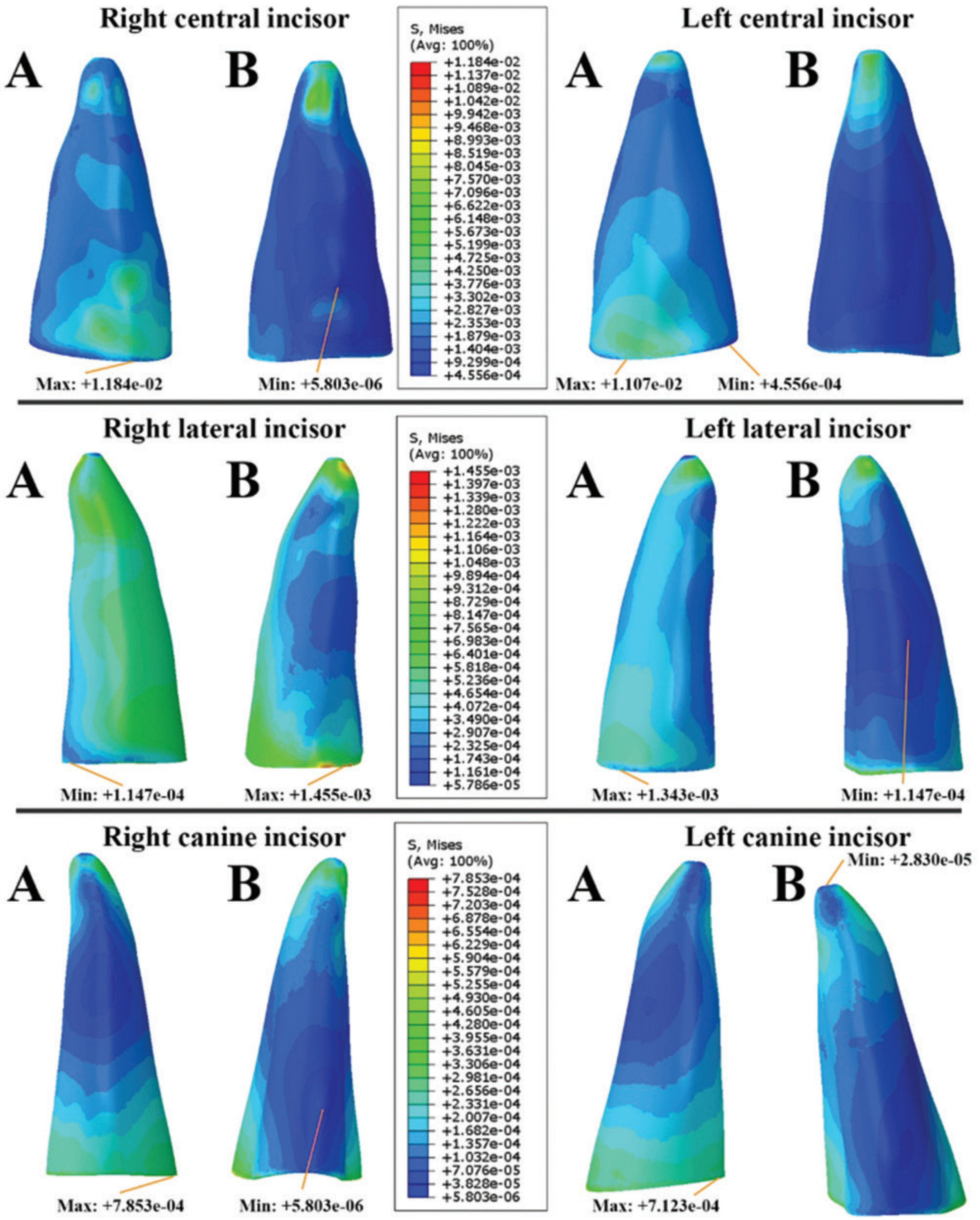

รูปที่ 4 *แผนภาพสีแสดงการกระจายความเครียดในฟันแต่ละซี่ เมื่อได้รับแรง 60 กรัมในหลักยึดแบบที่ 1 ด้านใกล้ริมฝีปาก (A) ด้านใกล้เพดาน (B)*

Figure 4 *Color-coded map showing the distribution of stress of 60 g force in each tooth in anchorage pattern 1: labial (A) and palatal (B).*

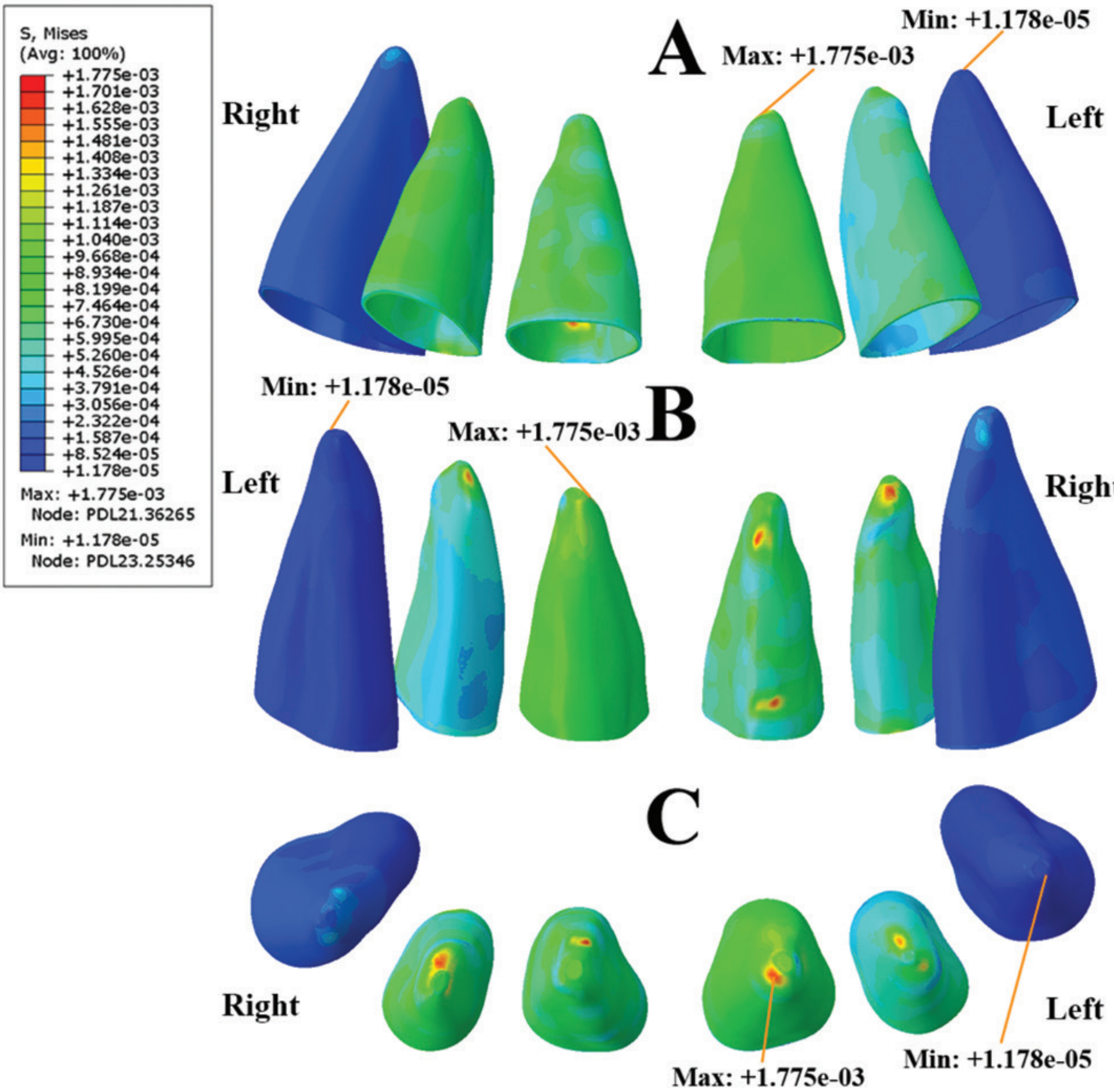

รูปที่ 5 *หลักยึดแบบที่ 2 แผนภาพสีแสดงการกระจายความเครียด เมื่อได้รับแรง 60 กรัม ด้านใกล้ริมฝีปาก (A) ด้านใกล้เพดาน (B) ด้านปลายราก (C)*

Figure 5 *Anchorage pattern 2, color-coded map showing the distribution of stress of 60 g force: labial (A), palatal (B), and apical views (C).*

Results

In anchorage pattern 1, the von Mises stress distribution was greater on the central incisors than on the lateral incisors or canines. The greatest stress value was found at the cervix of the labial side of the PDL of the right central incisor ($+1.184 \times 10^{-2}$ MPa). The least stress value was found at the cervical-middle third of the palatal side of the PDL of the right canine ($+5.803 \times 10^{-6}$ MPa) (Figure 3). There was much greater stress on the central incisors than on the lateral incisors or canines. The stress distribution pattern in each tooth is shown in Figure 4.

In anchorage pattern 2, the stress was greater on the central and lateral incisors than on the canines.

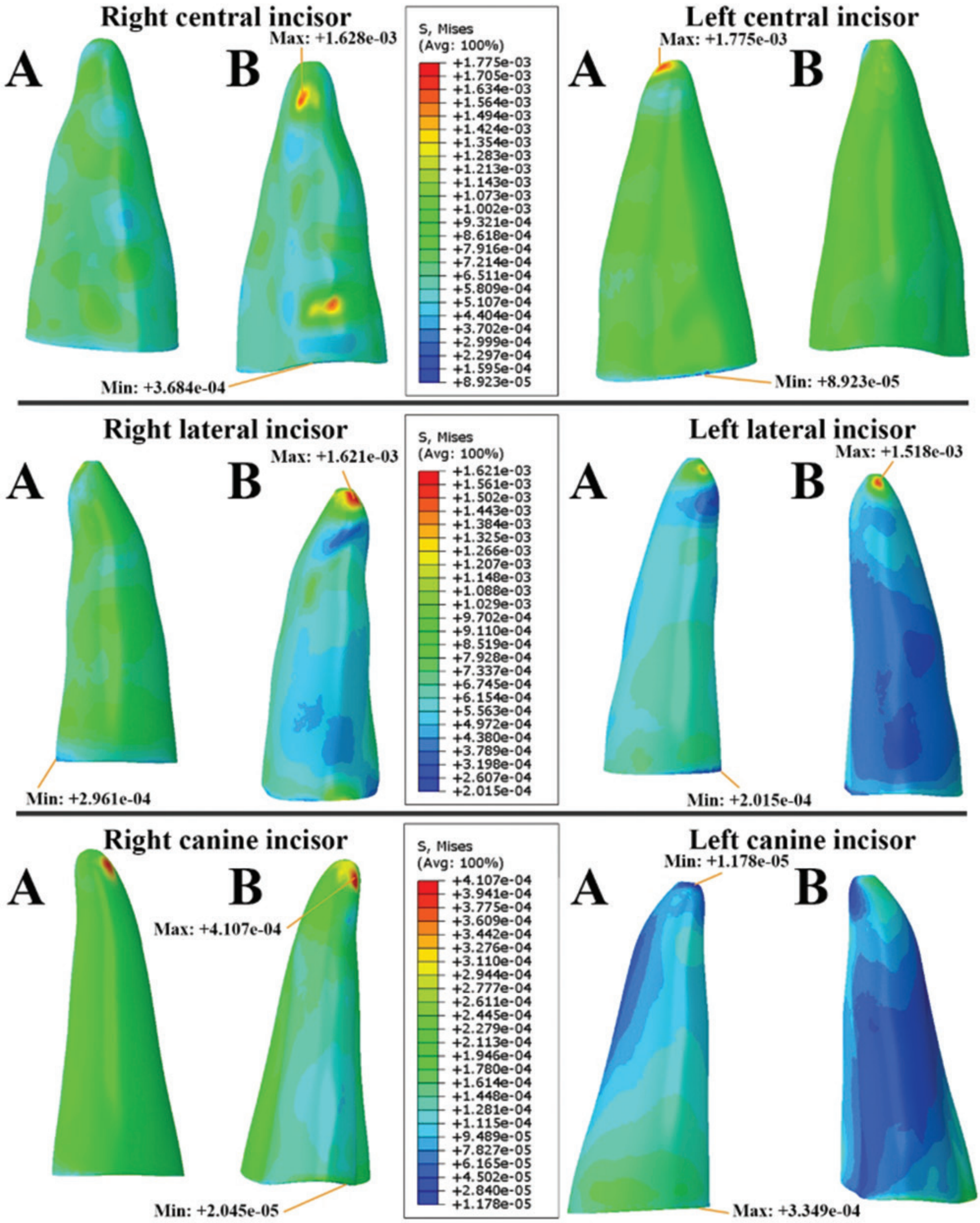

รูปที่ 6 *แผนภาพสีแสดงการกระจายความเครียดในฟันแต่ละซี่ เมื่อได้รับแรง 60 กรัมในหลักยึดแบบที่ 2 ด้านใกล้ริมฝีปาก (A) ด้านใกล้เพดาน (B)*

Figure 6 *Color-coded map showing the distribution of stress of 60 g force on each tooth of anchorage pattern 2: labial (A), palatal views (B).*

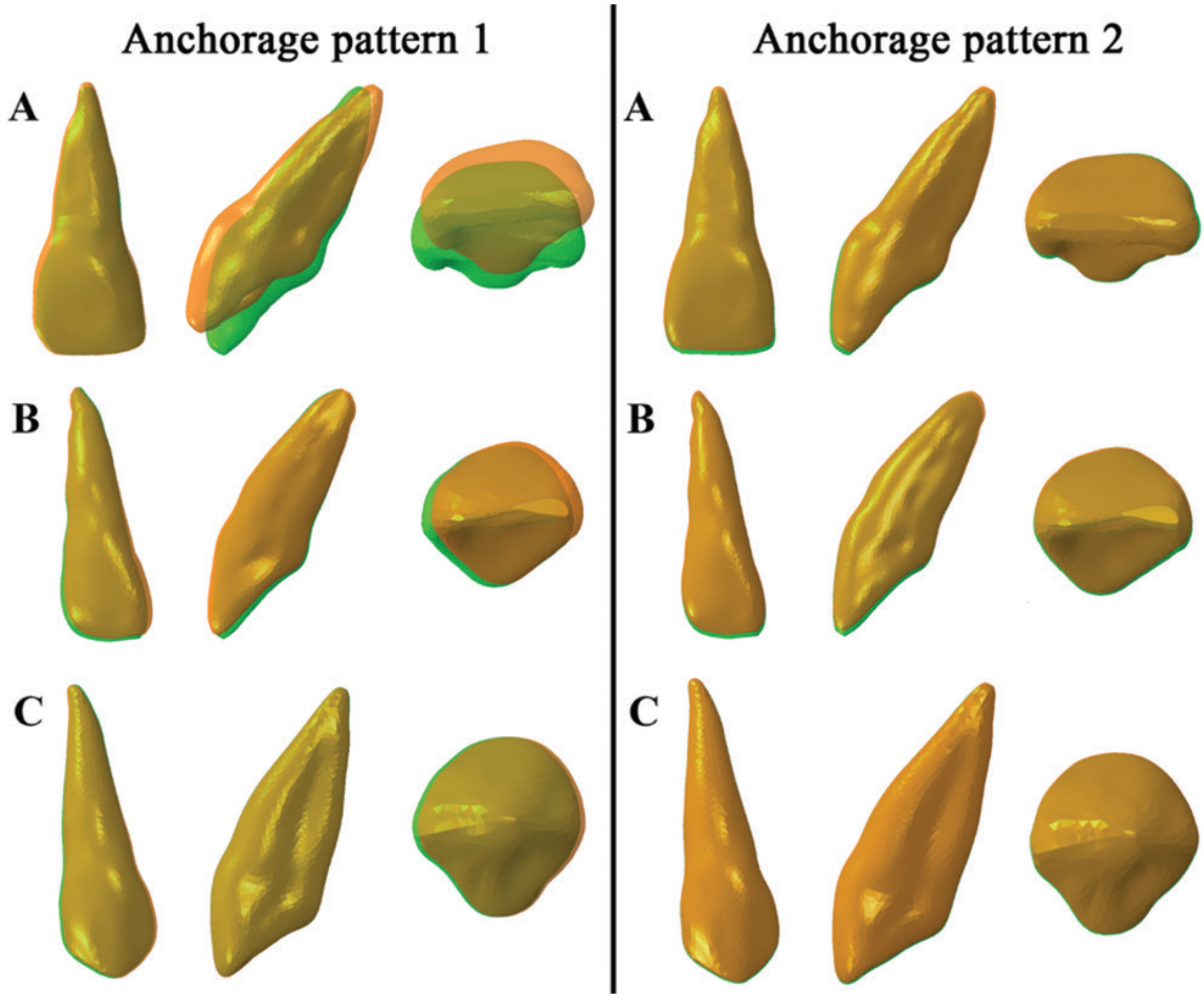

รูปที่ 7 *ภาพเปรียบเทียบการเคลื่อนที่ของฟัน ก่อน(สีเขียว) และ หลัง(สีส้ม) จากได้รับแรง (มีการขยายความแตกต่างให้มากขึ้น) แต่ละชุดของภาพประกอบด้วย ด้านใกล้ริมฝีปาก ด้านใกล้กลาง และด้านบดเคี้ยวของฟัน ตามลำดับ ฟันตัดซี่กลางด้านขวา (A) ฟันตัดซี่ข้างด้านขวา (B) ฟันเขี้ยวด้านขวา (C)*

Figure 7 *Displacement of teeth indicated by superimposition of before (green) and after (orange) loads of the teeth (Magnified differentiation). Each set of pictures consists of the labial, mesial and occlusal views, respectively. Right central incisor (A). Right lateral incisor (B). Right Canine (C).*

The greatest stress value was found at the apex of the PDL of the left central incisor (+1.775x10-3 MPa). The least stress value was found at the apex of the PDL of the left canine (+1.178x10-5 MPa) (Figure 5). There was rather equal on the central and lateral incisors and more than on the canines. The stress distribution pattern in each tooth is shown in Figure 6.

Displacement of the crowns and roots of the six maxillary anterior teeth in anchorage pattern 1 is shown in Table 3. In the x-axis, the mesio-distal direction, the crowns of the six maxillary teeth moved mesially and the root apices moved distally. In the y-axis, the vertical direction, the crowns and root apices of all teeth were intruded, except that the root apices of the canines were slightly extruded. In the z-axis, the labio-palatal direction, the crowns of all teeth moved labially, and the root apices of all teeth moved palatally. The central incisors moved farther than the lateral incisors or canines. The displacement of each tooth is shown in Figure 7.

Displacement of the crowns and roots of the six maxillary anterior teeth in anchorage pattern 2 is shown in Table 4. In the mesio-distal direction, the crowns of the six maxillary teeth moved distally and the root apices moved mesially. In the vertical direction, the crowns and root apices of all teeth were intruded. In the labio-palatal direction, the crowns of the central incisors moved palatally, whereas the crowns of the lateral incisors and canines moved

ตารางที่ 3 *การเคลื่อนที่ของฟันแต่ละซี่ในหลักยึดแบบที่ 1*

Table 3 *Displacement of each tooth in anchorage pattern 1*

Tooth	Part	Displacement (mm)		
		ΔX	ΔY	ΔZ
Right central incisor	Crown	2.06E-3	8.40E-3	6.98E-3
	Root	-1.51E-3	1.20E-3	-5.68E-3
Right lateral incisor	Crown	1.77E-3	1.24E-3	2.35E-3
	Root	-0.47E-3	0.30E-3	-1.59E-3
Right canine	Crown	1.02E-3	0.21E-3	1.20E-3
	Root	-0.41E-3	-6.97E-5	-0.44E-3
Left central incisor	Crown	-2.51E-3	8.22E-3	7.60E-3
	Root	1.64E-3	1.01E-3	-6.12E-3
Left lateral incisor	Crown	-1.26E-3	1.22E-3	1.70E-3
	Root	0.39E-3	0.18E-3	-1.07E-3
Left canine	Crown	-1.06E-3	4.30E-5	1.13E-3
	Root	0.48E-3	-0.25E-3	-0.28E-3

ตารางที่ 4 *การเคลื่อนที่ของฟันแต่ละซี่ในหลักยึดแบบที่ 2*

Table 4 *Displacement of each tooth in anchorage pattern 2*

Tooth	Part	Displacement (mm)		
		ΔX	ΔY	ΔZ
Right central incisor	Crown	-0.33E-3	1.61E-3	-0.64E-3
	Root	0.43E-3	1.34E-3	-1.08E-3
Right lateral incisor	Crown	-7.76E-5	1.92E-3	0.41E-3
	Root	0.24E-3	1.26E-3	-1.41E-3
Right canine	Crown	-0.19E-3	0.61E-3	0.26E-3
	Root	0.20E-3	0.33E-3	-0.38E-3
Left central incisor	Crown	0.91E-3	1.91E-3	-0.85E-3
	Root	-0.61E-3	1.73E-3	-1.28E-3
Left lateral incisor	Crown	0.49E-3	1.69E-3	0.41E-3
	Root	-0.44E-3	0.88E-3	-1.13E-3
Left canine	Crown	0.60E-3	0.30E-3	2.89E-5
	Root	-0.27E-3	7.53E-5	-0.18E-3

labially. The root apices of all teeth moved palatally. The central and lateral incisors moved a similar distance to each other, but a greater distance than the canines. The displacement of each tooth is shown in Figure 7.

Discussion

In anchorage pattern 1, the von Mises stress was more concentrated on the central incisors than on the lateral incisors or canines, whereas in anchorage pattern 2, the stress was concentrated on both the central and lateral incisors. There was less stress on the canines than on the central and lateral incisors in both anchorage patterns. The distribution of stress was greater on the teeth that were closer to the force application points. The greatest stress possible in anchorage pattern 1 ($+1.184 \times 10^{-2}$ MPa) was greater than that in anchorage pattern 2 ($+1.775 \times 10^{-3}$ MPa) due to the division of force. Since the net forces in both anchorage patterns were equal, the stress of 60-g force in anchorage pattern 1 was focused on a single point, whereas in anchorage pattern 2, the force was divided between F_L and F_R. Therefore, in anchorage pattern 2, the stress was better distributed. In addition to the points concluded above, the apices of the incisors received great stress, a finding which was consistent with the findings of previous studies(19,20), which stated that the area around the apices of the incisors was the most prone to resorption, especially the lateral incisors.(21-23)

The anterior teeth are usually proclined when they are intruded. In this study, the stress distribution and displacement of the teeth suggest that the teeth would be proclined if anchorage pattern 1 were to be used in the clinical setting. However, in anchorage pattern 2, the lateral incisors and canines were slightly proclined, but the central incisors were intruded along the long axis. Other FEM studies also reported the proclination of the intruded incisors.(19,20) Saga *et al*(20) reported a strong tendency towards proclination of the maxillary central incisors when the point of force application was more anterior. Park *et al*.(10) reported that equal stress distribution and pure intrusion of the six mandibular anterior teeth occurred when mini-screws were placed distal to the canines and the force applications were between the central and lateral incisors. Our results have shown that an oblique force, as used in anchorage pattern 2, leading to pure intrusion of the anterior teeth. The oblique force consists of the combined forces of the palatal and intrusive vertical force vectors. The vector of force in the palatal direction resisted the proclination of the teeth, so the teeth in anchorage pattern 2 were intruded along their long axes.

The central incisors in anchorage pattern 1 moved a greater distance than those in anchorage pattern 2 due to the difference in stress distribution in the two patterns. In anchorage pattern 1, the distribution was concentrated in the central incisors, which were closest to the force application point. Thus, the central incisors in anchorage pattern 1 moved the greatest distance. Anchorage pattern 2, however, had two force application points, which is why the stress was distributed among the four teeth, central and lateral incisors. Therefore, the central incisors in anchorage pattern 2 moved a shorter distance than those in anchorage pattern 1, but the lateral incisors and canine in anchorage pattern 2 moved a greater distance. These results show that the force application point affected the stress distribution on each tooth. With equal force, teeth that were closer to the force application point had greater stress distribution, resulted in greater displacement.

In FEM studies, the reliability of the results depends on the accuracy of the model. This study had some limitations. The PDL and cortical bone were created with uniform thickness. In reality, however, the PDL and the cortical bone are not of uniform thickness.(15,24,25) Friction between teeth is also another factor relating to the magnitude of force applied for tooth intrusion. However, this study applied no friction between neighboring teeth. The first premolar was not created in the FE model, which was another limitation. Additionally, all materials, (except the PDL, whose property, according to previous studies[24,26-28] is non-linear) were assigned with linear elastic properties.

Further study is needed to determine the effect of treatment time on the movement of teeth. In clinical settings over long periods of time, the movement of teeth would probably differ from the results in this study.

Conclusions

1. The stress in the two-mini-screw anchorage pattern was distributed widely over the four incisors, whereas the stress in the one-mini-screw anchorage pattern was concentrated only in the two central incisors.

2. When the net force in both anchorage patterns is equal, the greatest stress in the two-mini-screw pattern is less than that in the one-mini-screw pattern

3. The two-mini-screw anchorage pattern displaces the six maxillary anterior teeth closer to pure intrusion. The one-mini-screw anchorage pattern intrudes the teeth with proclination.

Acknowledgments

The authors would like to acknowledge Mr. Pattarapon Saigerdsri, Master degree student, Faculty of Engineering, Chiang Mai University, Thailand for his assistance in the use of the SolidWorks and Abaqus software during the research study, and Dr. M. Kevin O. Carroll, Professor Emeritus of the University of Mississippi School of Dentistry, USA and Faculty Consultant at Chiang Mai University Faculty of Dentistry, Thailand, for language editing.

References

1. Burstone CR. Deep overbite correction by intrusion. *Am J Orthod* 1977; 72: 1-22.
2. Burstone CJ. Biomechanics of deep overbite correction. *Seminars in orthodontics* 2001; 7: 26-33.
3. Sreedhar C, Baratam S. Deep overbite-A review (Deep bite, Deep overbite, Excessive overbite). *Annals and Essences of Dentistry* 2009; 1: 8-25.
4. Jain RK, Kumar SP, Manjula WS. Comparison of intrusion effects on maxillary incisors among mini implant anchorage, j-hook headgear and utility arch. *J Clin Diagn Res* 2014; 8: ZC21-ZC24.
5. Polat-Ozsoy O, Arman-Ozcirpici A, Veziroglu F. Miniscrews for upper incisor intrusion. *Eur J Orthod* 2009; 31: 412-416.
6. Ohnishi H, Yagi T, Yasuda Y, Takada K. A mini-implant for orthodontic anchorage in a deep overbite case. *Angle Orthod* 2005; 75: 444-452.
7. Kim TW, Kim H, Lee SJ. Correction of deep overbite and gummy smile by using a mini-implant with a segmented wire in a growing Class II Division 2 patient. *Am J Orthod Dentofacial Orthop* 2006; 130: 676-685.
8. Upadhyay M, Nagaraj K, Yadav S, Saxena R. Mini-implants for en masse intrusion of maxillary anterior teeth in a severe Class II division 2 malocclusion. *J Orthod* 2008; 35: 79-89.
9. Nanda RS, Tosun Y. *Biomechanics in orthodontics: Principles and Practice*. Hanover Park, IL, USA: Quintessence Publishing Co; 2010.
10. Park HK, Sung EH, Cho YS, Mo SS, Chun YS, Lee KJ. 3-D FEA on the intrusion of mandibular anterior segment using orthodontic miniscrews. *Korean Assoc Orthod* 2011; 41: 384-398.
11. Konda P, Tarannum S. Basic principles of finite element method and its applications in orthodontics. *J Pharm Biomed Sci* 2012; 16: 1-8.

12. Ansari T, Mascarenhas R, Paulose V. Trends in orthodontics...finite element analysis and its applications in orthodontics. *APOS-Trends Orthod* 2011; 2: 5-9.
13. Kojima Y, Kawamura J, Fukui H. Finite element analysis of the effect of force directions on tooth movement in extraction space closure with miniscrew sliding mechanics. *Am J Orthod Dentofacial Orthop* 2012; 142: 501-508.
14. Caballero GM, Carvalho Filho OA, Hargreaves BO, Brito HH, Magalhaes Jr PA, Oliveira DD. Mandibular canine intrusion with the segmented arch technique: A finite element method study. *Am J Orthod Dentofacial Orthop* 2015; 147: 691-697.
15. Choi JH, Yu HS, Lee KJ, Park YC. Three-dimensional evaluation of maxillary anterior alveolar bone for optimal placement of miniscrew implants. *Korean J Orthod* 2014; 44: 54-61.
16. Cifter M, Sarac M. Maxillary posterior intrusion mechanics with mini-implant anchorage evaluated with the finite element method. *Am J Orthod Dentofacial Orthop* 2011; 140: e233-e241.
17. Huang H, Tang W, Yan B, Wu B. Mechanical responses of periodontal ligament under a realistic orthodontic loading. *Procedia Eng* 2012; 31: 828-833.
18. Proffit WR, Fields HW, Sarver DM. *The biologic basis of orthodontic therapy. contemporary orthodontics*. 5th ed. St. Louis, MO, USA: Elsevier/Mosby; 2013: 286-287.
19. Salehi P, Gerami A, Najafi A, Torkan S. Evaluating stress distribution pattern in periodontal ligament of maxillary incisors during intrusion assessed by the finite element method. *J Dent (Shiraz)* 2015; 16: 314-322.
20. Saga AY, Maruo H, Argenta MA, Maruo IT, Tanaka OM. Orthodontic intrusion of maxillary incisors: a 3D finite element method study. *Dental Press Inter* 2016; 21: 75-82.
21. Artun J, Smale I, Behbehani F, Doppel D, Van't Hof M, Kuijpers-Jagtman AM. Apical root resorption six and 12 months after initiation of fixed orthodontic appliance therapy. *Angle Orthod* 2005; 75: 919-926.
22. Mohandesan H, Ravanmehr H, Valaei N. A radiographic analysis of external apical root resorption of maxillary incisors during active orthodontic treatment. *Eur J Orthod* 2007; 29: 134-139.
23. Yu JH, Shu KW, Tsai MT, Hsu JT, Chang HW, Tung KL. A cone-beam computed tomography study of orthodontic apical root resorption. *J Dent Sci* 2013; 8: 74-79.
24. Toms SR, Eberhardt AW. A nonlinear finite element analysis of the periodontal ligament under orthodontic tooth loading. *Am J Orthod Dentofacial Orthop* 2003; 123: 657-665.
25. Baumgaertel S, Hans MG. Buccal cortical bone thickness for mini-implant placement. *Am J Orthod Dentofacial Orthop* 2009; 136: 230-235.
26. Toms SR, Lemons JE, Bartolucci AA, Eberhardt AW. Nonlinear stress-strain behavior of periodontal ligament under orthodontic loading. *Am J Orthod Dentofacial Orthop* 2002; 122: 174-179.
27. Natali AN, Pavan PG, Scarpa C. Numerical analysis of tooth mobility: formulation of a non-linear constitutive law for the periodontal ligament. *Dent Mater* 2004; 20: 623-629.
28. Shibata T, Botsis J, Bergomi M, Mellal A, Komatsu K. Mechanical behavior of bovine periodontal ligament under tension-compression cyclic displacements. *EJOS* 2006; 114: 74-82.

Faculty of Dentistry
Chiang Mai University

Cleft Center

Dental Hospital, Faculty of Dentistry, Chiang Mai University

From Cleft to Sm:)e

by our hearts

For more information or donation please contact
Department of Orthodontics and Pedodontics
Faculty of Dentistry, Chiang Mai University
Tel. 053-944464-65